"Next-Generation Semiconductors for Solar Photoelectrolysis", FINAL REPORT

Peter Khalifah, Stony Brook University

1. $(GaN)_{1-x}(ZnO)_x$

The $(GaN)_{1-x}(ZnO)_x$ solid solution has previously been demonstrated to be the single-semiconductor system with the highest external quantum efficiency for driving overall water splitting with visible light using suspended particles. However, the efficiency for this process is not fully optimized (~6%) and can potentially be increased by an order of magnitude or more.

1.1 Improved synthesis of $(GaN)_{1-x}(ZnO)_x$

While the initial characterization of the $(GaN)_{1-x}(ZnO)_x$ system by others focused on the Ga-rich end of the solid solution, the Zn-rich end of this solid solution has the expected advantages of better visible light absorption and lower materials cost. To date, Zn-rich $(GaN)_{1-x}(ZnO)_x$ phases have been minimally characterized due to synthetic challenges associated with producing these phases in bulk amounts with a controlled composition. We have demonstrated that a modified layered double hydroxide (LDH) synthesis method in which the vapor pressure of Zn is controlled eliminates the problem of rapid Zn evaporation and allows the facile preparation of Zn-rich $(GaN)_{1-x}(ZnO)_x$ phases with the same cation ratio as the starting precursors across a wide range of compositions ($0.20 < x < 0.95$). Optical studies have been carried out on these samples, and it is found that a minimum direct gap of about 2.6 eV occurs near $x = 0.6$. This represents an unprecedented degree of synthetic control for this system, and the first chance to characterize the evolution of properties for this system using a series of similarly prepared samples.

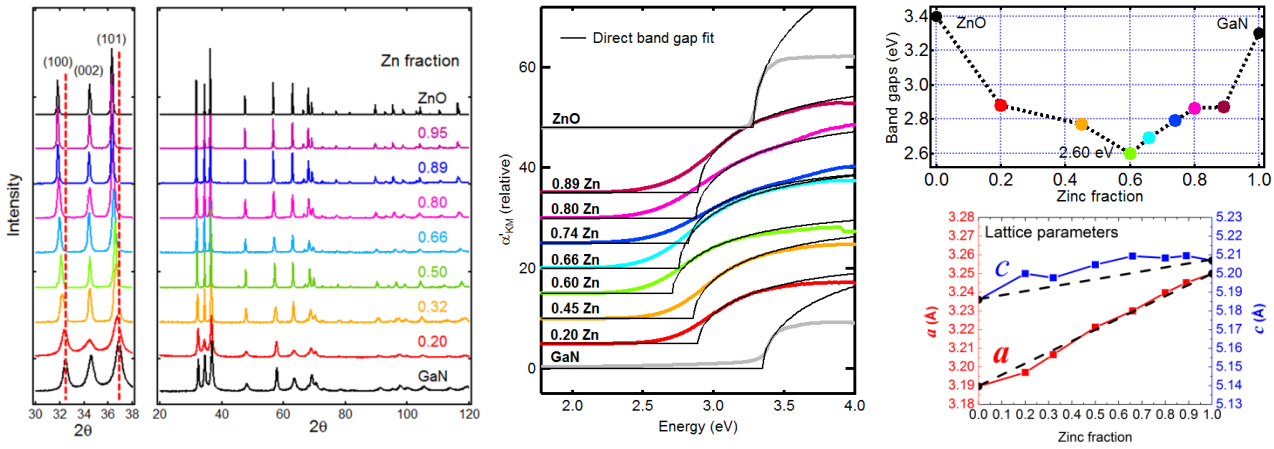

Figure 1.1. Plots of X-ray diffraction patterns (left) and relative absorption spectra obtained from the Kubelka-Munk transform of diffuse reflectance data (center) for $(GaN)_{1-x}(ZnO)_x$ semiconductors spanning a very wide range of compositions, together with the direct optical gaps and the lattice parameters obtained by fitting this data.

1.2 Discovery of stacking faults in $(GaN)_{1-x}(ZnO)_x$

Despite the sharp diffraction peaks for $(GaN)_{1-x}(ZnO)_x$ semiconductors which can be fully indexed using the simple hexagonal wurtzite structure type, we have discovered that many synthesis methods for these semiconductors lead to the formation of coherent cubic intergrowths within the hexagonal lattice. We have developed new diffraction and structural analysis methods for quantitatively modeling the contribution of these intergrowths. In a representative sample of $(GaN)_{1-x}(ZnO)_x$ with $x = 0.35$, we have demonstrated that the cubic intergrowths are 4 layers wide, and that 9% of the close-packed layers are in a cubic rather than a hexagonal arrangement.

These cubic intergrowths represent a non-polar domain within the polar wurtzite structure, and may therefore be expected to strongly influence the separation of photogenerated charges within this system. It is found that the presence or absence of cubic domains is driven by kinetic and not thermodynamic forces as their abundance depends on the synthesis procedure. Our new LDH method does not produce cubic intergrowths, in contrast to classic syntheses from oxide structure precursors (such as Ga_2O_3 or $ZnGa_2O_4$) which have pre-existing close-packed domains.

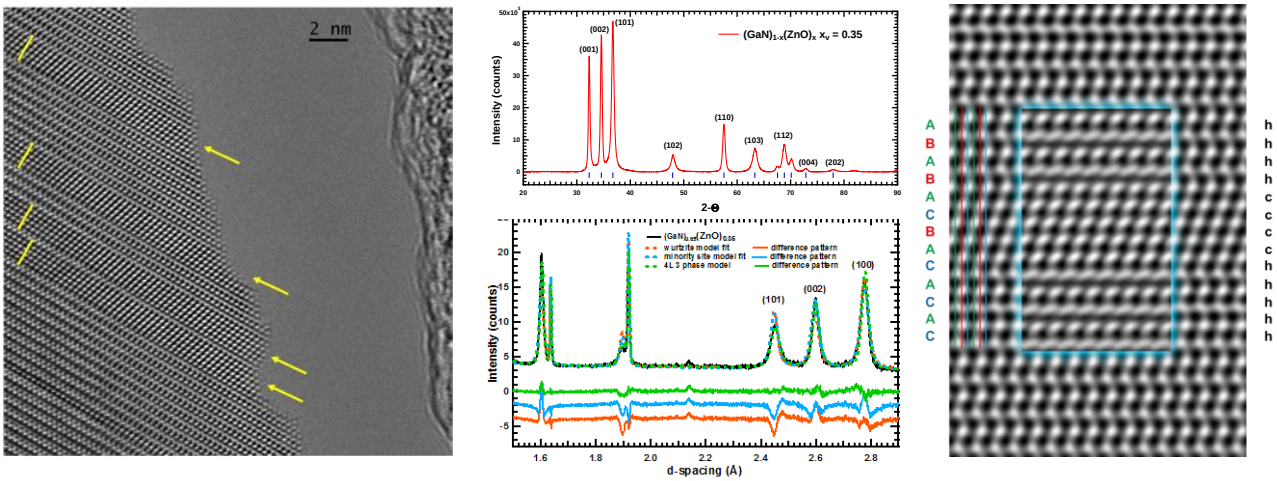

Figure 1.2. Left: Direct TEM evidence of cubic intergrowths of a consistent width (marked with yellow lines) in a $(GaN)_{1-x}(ZnO)_x$ sample with $x = 0.35$. Center: Although laboratory X-ray diffraction patterns of this sample can be completely indexed using the conventional wurtzite unit cell (top panel), the intensity of the diffraction peaks cannot be effectively fit unless an extended *c*-axis superstructure is used to model the structure of this compound (bottom panel), as can be seen in the much flatter difference pattern using a $c \sim 300$ Å supercell (green) instead of the conventional $c \sim 5$ Å wurtzite structure with (blue) or without (red) additional minority sites corresponding to the positions of atoms in faulted layers. Right: The 4-layer width of cubic intergrowths inferred from fits to diffraction data is confirmed by the match between observed (center) and simulated (exterior) TEM images.

1.3 Estimation of absolute optical constants for $(GaN)_{1-x}(ZnO)_x$

Despite more than 10 years of intensive study, the absolute absorption coefficients for $(GaN)_{1-x}(ZnO)_x$ semiconductors have not previously been reported, primarily due to the lack of a simple method for measuring the absolute optical constants of powder samples. We have in the course of this project developed self-referenced reflectance spectroscopy as a new technique that can be generally used to determine the absolute optical constants for semiconductor powders, and have carried out pioneering studies on well-known semiconductors to validate this approach. In order to calculate absolute absorbances from powder reflectance data, it is necessary to accurately determine both the sample refractive index, $n(E)$, and to accurately determine the particle size of the powders, D. Both experimental and theoretical estimates of $n(E)$ for $(GaN)_{1-x}(ZnO)_x$ powders have been carried out, and these results were found to be generally consistent with each other and with prior optical studies of the end members, GaN and ZnO. A 3-parameter Sellmeier equation was found to be very useful in simply describing the energy-dependence of $n(E)$. Using these results together with various techniques for particle size analysis, we succeeded in making the first good estimates of the absolute absorption coefficients of $(GaN)_{1-x}(ZnO)_x$ semiconductors. The absorption of these compounds is not particularly strong, and the modest absorption coefficient of $\alpha \sim 10^4$ cm^{-1} at 3 eV is suggests that incomplete light absorption substantially contributes to the low quantum efficiencies previously measured

for this system by other groups, very consistent with their observation that the quantum efficiency for water splitting scales linearly with absorption for $(GaN)_{1-x}(ZnO)_x$ powders.

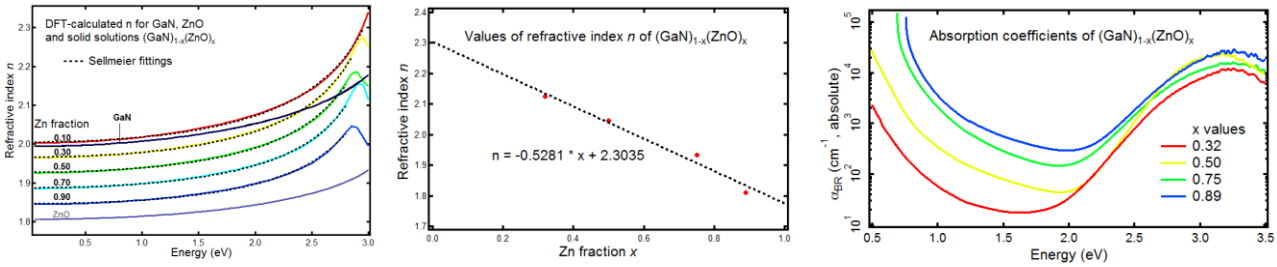

Figure 1.3. Left: Refractive index of $(GaN)_{1-x}(ZnO)_x$ calculated from first-principles DFT (colored lines) with the below-gap response fit to a 3-parameter Sellmeier equation (solid black lines). Center: Refractive index of $(GaN)_{1-x}(ZnO)_x$ powder samples determined using a novel self-referenced method through single-parameter (constant-valued) fits. Right: Absolute absorption coefficients of $(GaN)_{1-x}(ZnO)_x$ samples estimated from experimentally determined refractive indices and particle size distribution.

1.4 Control over free carrier concentration of $(GaN)_{1-x}(ZnO)_x$

It was been previously demonstrated that the quantum efficiency for overall water splitting of $(GaN)_{1-x}(ZnO)_x$ semiconductors can be significantly enhanced (2X) by a post-synthesis annealing treatment in air at modest temperatures, though the origin for this enhancement was not elucidated in that report. We postulated that the change in carrier concentration introduced by thermal annealing was the dominant reason for the change in photoactivity, and we therefore searched for methods to directly quantify and control the free carrier concentration in $(GaN)_{1-x}(ZnO)_x$ semiconductors with the goal of being able to directly control photoactivity by varying the free carrier concentration. In this work, we have shown that the diffuse reflectance measurements at infrared energies (0.5 – 1.5) show a very strong absorption feature (stronger than absorption across the band gap) which allows changes in the free carrier concentration to be easily followed. Furthermore, we have used EPR spectroscopy to show that the magnitude of this low-energy absorption is directly proportional to the free carrier concentration, which can change by two orders of magnitude or more during thermal annealing.

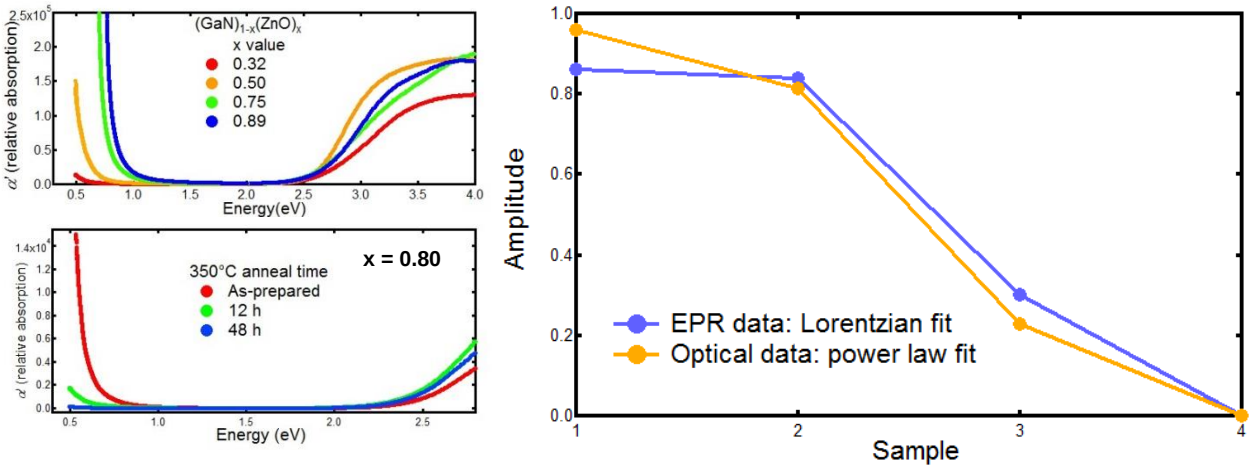

Figure 1.4a. Left top: The low-energy (0.5 – 1.5 eV) optical signature of free carriers is present in $(GaN)_{1-x}(ZnO)_x$ samples with a wide range of concentrations, though the response is strongest for the most Zn-rich samples. Left bottom: The free carrier concentration can be gradually reduced when samples are annealed in air at modest temperatures. Right: The magnitude of the optical response at low energies (0.5 – 1.5 eV) scales proportionally with the magnitude of the sample EPR signal, which is a direct measure of the unpaired spins of free carriers.

This work demonstrates the importance of below-gap measurements of the optical response of semiconductors for solar water splitting, a measurement regime which has been ignored in prior studies. Furthermore, this simple optical probe allows the origins of the changes in free carrier concentration to be systematically investigated using both indirect and direct measurements. Oxidation is a critical driving force for the changes that occur during thermal annealing as the infrared absorption is only suppressed by atmospheres which are strongly (O_2, air) or weakly (N_2, Ar) oxidizing, and not by atmospheres which are strongly reducing (H_2, NH_3) due to the presence of chemical moieties which actively scavenge oxygen. Thermogravimetric analysis (TGA) measurements indicate that annealing conditions which suppress the infrared free carrier absorption also lead to a small sample mass gain, as is expected for the replacement of 1 N^{3-} anion with 1.5 O^{2-} anions. The oxidation of 2 N^{3-} to 1 N_2 can be directly confirmed in neutron pair distribution function measurements which show the appearance of a new peak at the N≡N bond length of 1.1 Å after thermal annealing, indicating that N_2 gas formed through the thermal oxidation of the semiconductor is expelled from the lattice but remains trapped in the solid.

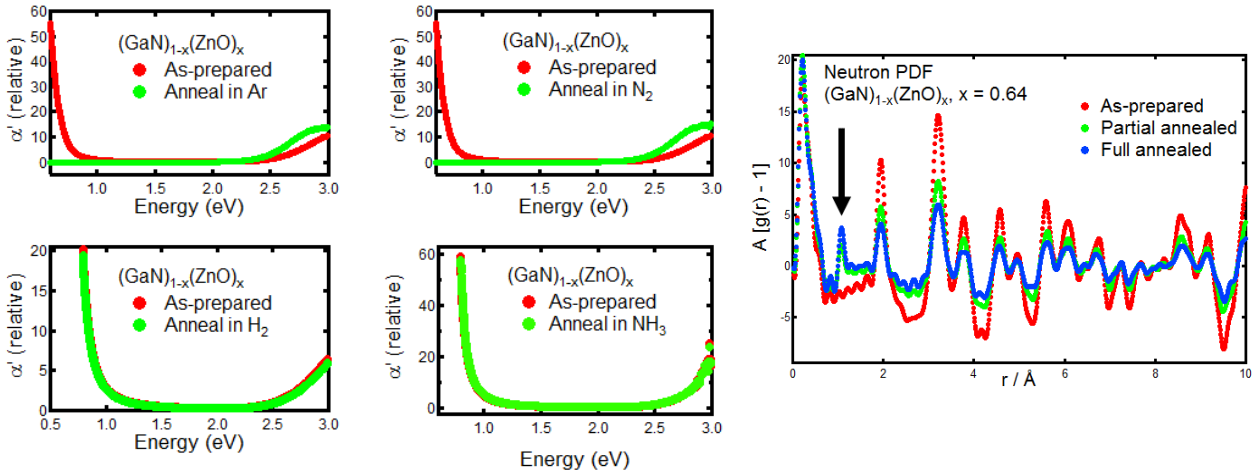

Figure 1.4b. Left: The low-energy absorption of $(GaN)_{1-x}(ZnO)_x$ samples is suppressed by annealing at temperatures of ~500 °C in atmospheres that contain O_2 at ppm levels (Ar, N_2) but is not changed during annealing at similar temperatures under actively reducing environments (5% H_2, NH_3), confirming that oxidative processes are needed to reduce the carrier concentration in as-prepared samples of $(GaN)_{1-x}(ZnO)_x$. The native carriers can therefore be concluded to be electrons. Right: The partial or complete suppression of the free carrier absorption in $(GaN)_{1-x}(ZnO)_x$ semiconductors is accompanied by the oxidation of lattice N^{3-} anions to N_2 gas which remain trapped in the solid, as can be seen in the new peak that occurs in neutron pair distribution function (PDF) data after samples have been annealed at the 1.1 Å distance expected for N≡N bonds.

Our newfound ability to control the carrier concentration of $(GaN)_{1-x}(ZnO)_x$ semiconductors allows the influence of free carrier concentration on photoactivity to be probed. Due to the termination of this project, only limited photoelectrochemical studies have been carried out. These studies on coated films of powders on a transparent conducting electrode were focused on a single composition (x = 0.64) which has one of the smallest band gaps for this system, and which is much more Zn-rich than semiconductors in this solid solution which were previously studied. The as-prepared semiconductor exhibited a significant photocurrent for water oxidation when functionalized with a RuO_2 co-catalyst. Annealing treatments which resulted in the complete suppression of the free carrier absorption also resulted in the essentially complete suppression of photoactivity. Complex behavior was seen for samples whose free carrier concentration was partially reduced by thermal annealing, with both the magnitude of the

photocurrent and the rapidity of the onset of the photocurrent depending on the carrier concentration in a non-monotonic fashion. These measurements clearly indicate that the free carrier concentration is an important parameter which strongly influences the photochemical activity of this semiconductor system, though more detailed follow-up studies are needed to better understand the optimal carrier concentration for photoactivity as well as its composition dependence. The tools that we have developed for quantifying and controlling the free carrier concentration in this system can be effectively deployed in future experiments over a wider range of semiconductor compositions and solution environments to gain this understanding.

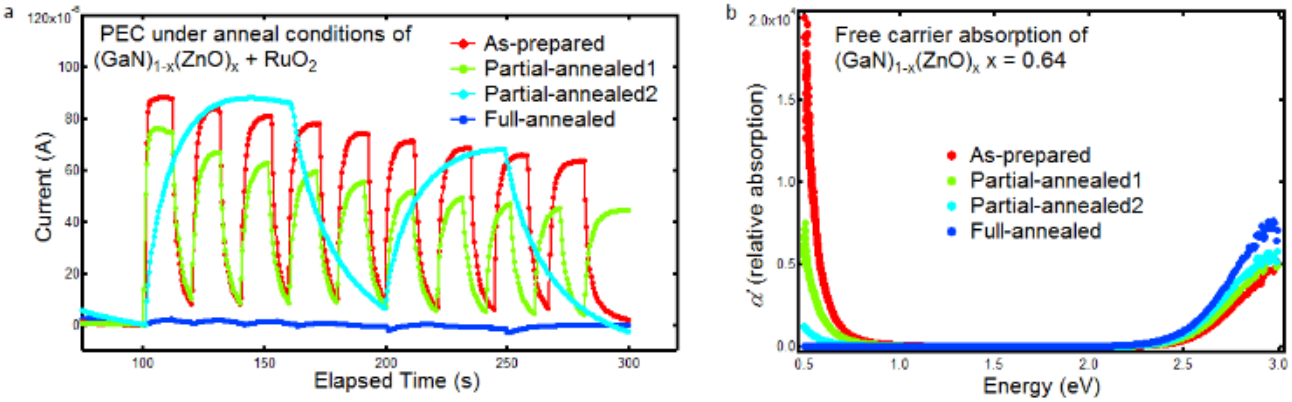

Figure 1.4c. Changes in photoactivity (left) and infrared absorption associated with free carriers (right) for a sample of $(GaN)_{1-x}(ZnO)_x$ with x = 0.64 annealed at different conditions to reduce the native concentration of free carriers. Measurements of RuO_2-functionalized semiconductor powder films were carried out at an applied potential of 0.5 V vs Ag/AgCl in an 0.5 M electrolyte of Na_2SO_4 buffered to a pH of 4.5.

In summary, we have developed a suite of both synthetic and analytical tools that allow unprecedented ability to prepare, evaluate, and rationally optimize the suitability of complex wurtzite $(GaN)_{1-x}(ZnO)_x$ semiconductors for solar fuel production. Many of these approaches – such as the use of infrared spectroscopy to assess free carrier concentrations and the use of novel bidirectional reflectance techniques to obtain the absolute optical coefficients of powder samples – can be broadly applied to the study of semiconductor samples for solar water splitting. These efforts represent an important conceptual shift to move away from assuming that semiconductors are fully stoichiometric (as is routinely done in the literature in this field), and to instead work on quantifying and controlling the doping level of the complex emerging semiconductors being considered for solar fuel production despite the dearth of tools for doing so. This work will be divided into 5 manuscripts. One has already been submitted. The other four have all been written as chapters in the recently defended Ph. D. thesis of Huafeng Huang, and will be submitted for publication shortly.

2. $LaTiO_2N$

The direct optical gap of $LaTiO_2N$ is about 2.2 eV and thus falls within the range of optimal band gaps for *Z*-scheme (2-semiconductor) solar water splitting, in contrast to $(GaN)_{1-x}(ZnO)_x$, whose minimum direct gap of ~2.6 eV is too small to ever allow solar water splitting with a sufficient overall efficiency suitable for practical applications (> 10%). As such, $LaTiO_2N$ is a more desirable candidate photoanode than $(GaN)_{1-x}(ZnO)_x$, though $LaTiO_2N$ has a far more chemically complex structure than that wurtzite structure of $(GaN)_{1-x}(ZnO)_x$ and is therefore a much more challenging target to develop for photoelectrochemical applications.

2.1 Epitaxial $LaTiO_2N$ film photoanodes

In prior work, we used spectral ellipsometry to show that the absolute absorption coefficient of $LaTiO_2N$ reaches 10^5 cm^{-1} by 2.5 eV, only about 0.25 eV in energy higher than the previously reported band gap of this phase. This is both of fundamental interest (represents the most rapid onset of strong visible light absorption for any known semiconductor) and of practical interest (it suggests that the optimum photoelectrode thickness for this phase is only 100 – 200 nm, about an order of magnitude less than PVD $LaTiO_2N$ films previously examined by other groups. While the preparation of epitaxial $LaTiO_2N$ on top of highly insulating $La_2Ti_2O_7$ single crystals was previously demonstrated by others, we were the first to show that epitaxial $LaTiO_2N$ films can be prepared on top of back, conductive $La_5Ti_5O_{17}$ single crystals that can serve as the back electrode during photoelectrochemical testing. In this project, we have worked to develop methods for preparing high-quality epitaxial films of $LaTiO_2N$ of controlled thickness that will have optimal photoelectrochemical performance.

The first step in this work was to carry out the growth of large single crystals of $La_5Ti_5O_{17}$ using a specialized optical floating zone furnace. These crystals could be cleaved to form flat surfaces with areas of up to ~1 cm^2, and it was verified through X-ray diffraction studies that crystalline $LaTiO_2N$ films could be grown on top of the cleaved substrate, and through spectral ellipsometry measurements that the optical properties of $LaTiO_2N$ on conductive $La_5Ti_5O_{17}$ were indistinguishable from those on alternate substrates. Appropriate reaction conditions were identified for growing epitaxial $LaTiO_2N$ films with thicknesses ranging from 100 to 2000 nm, with the film thicknesses determined indirectly by spectral ellipsometry after calibrating this technique using direct TEM observations.

Figure 2.1a. Left: Epitaxial $LaTiO_2N$ thin films were prepared on top of substrates of transparent single crystals of insulating $La_2Ti_2O_7$ and on black single crystals of conductive $La_5Ti_5O_{17}$. Right: Diffraction patterns show the crystallographic co-alignment of perovskite $LaTiO_2N$ film peaks (110 and 220 when indexed to an idealized cubic cell) with the corresponding perovskite-like peaks of the more complex layered perovskite structure of substrates.

After bulk measurements confirmed that $LaTiO_2N$ films of desired thicknesses could be prepared on top of $La_5Ti_5O_{17}$ substrates, complimentary local scanning transmission electron microscopy (STEM) measurements with atomic resolution (< 1 Å) were used to assess and improve the quality of these films. Despite the sharp diffraction peaks from these $LaTiO_2N$ films, it was found that films generally had an amorphous surface layer that could be as much as 20 nm thick above the crystalline $LaTiO_2N$ phase. Scanning EELS measurements showed that the amorphous region had a substantially higher O:N ratio than the bulk $LaTiO_2N$ phase, suggesting that the formation of the amorphous region was triggered by a loss of nitrogen at low temperatures at which expected crystalline decomposition products (*e.g.* TiO_2) could not form due to the inability of ions to diffuse in the solid state at these temperatures. The loss of nitrogen was hypothesized to be triggered by the lower chemical potential of nitrogen at lower

temperatures (< 600 °C) at which the NH_3 gas used as a nitrogen source is less likely to fragment and produce reactive nitrogen species. This hypothesis was confirmed by studies on quenched samples, for which no evidence of a surface amorphous layer could be found in STEM images.

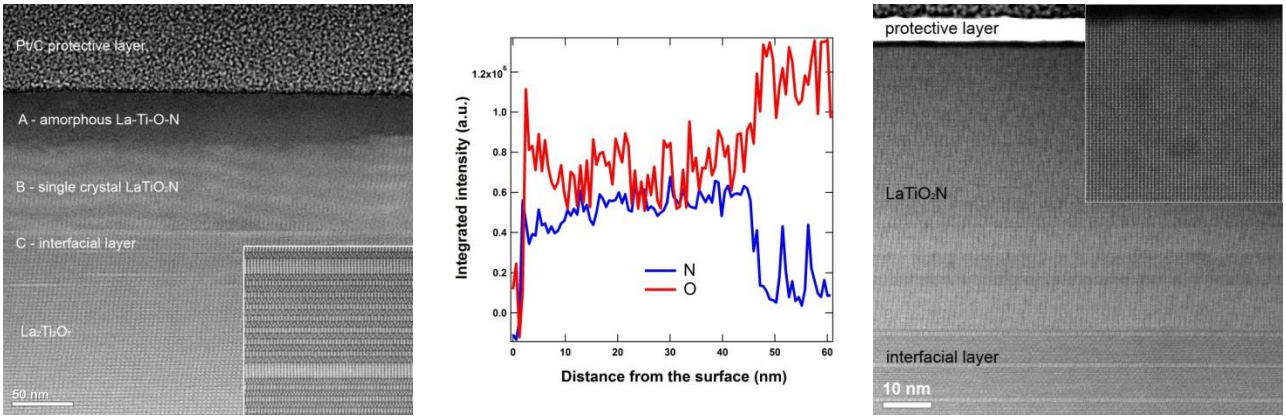

Figure 2.1b. Left: Cross-sectional TEM image of naturally cooled thin film of $LaTiO_2N$ on top of a $La_2Ti_2O_7$ single crystal substrates shows that there are four different layers rather than the expected two. From bottom to top, they are the $La_2Ti_2O_7$ substrate, an interfacial layer when the $LaTiO_2N$ and $La_2Ti_2O_7$ lattices are intergrown, a crystalline $LaTiO_2N$ layer, and an amorphous layer of decomposed $LaTiO_2N$. Center: chemical analysis of EELS spectra show that the amorphous layer is oxygen-rich relative to $LaTiO_2N$, consistent with the decomposition process involving the loss of N^{3-} ions from the lattice as N_2. Right: STEM images of thin films which are quenched instead of naturally cooled show no evidence of the surface amorphous layer.

The relationship between film preparation and photoactivity was further explored through photoelectrochemical measurements. Surprisingly, as-prepared films which were cooled without quenching exhibited an unexpected redox feature in cyclic voltammetry measurements, manifesting as an oxidation peak around 1 V *vs.* RHE and a reduction peak around 0.5 V *vs.* RHE. The reduction peak could only be observed if a prior oxidation sweep had been carried out, suggesting that this redox activity is associated with Ti^{3+} species that were generated during the surface decomposition reaction (N^{3-} anions oxidize to form N_2, driving a corresponding Ti^{4+} to Ti^{3+} reduction in the lattice). This feature was suppressed but was still present in quenched films, suggesting that surface decomposition still occurs even though amorphous regions could not be directly observed in atomic-scale STEM studies. However, the Ti^{4+}/Ti^{3+} redox feature could be eliminated if quenched films were mechanically polished to physically remove surface layers. These films had a very flat dark current in CV measurements, and represent the best film preparation to use for photoelectrochemical activity testing.

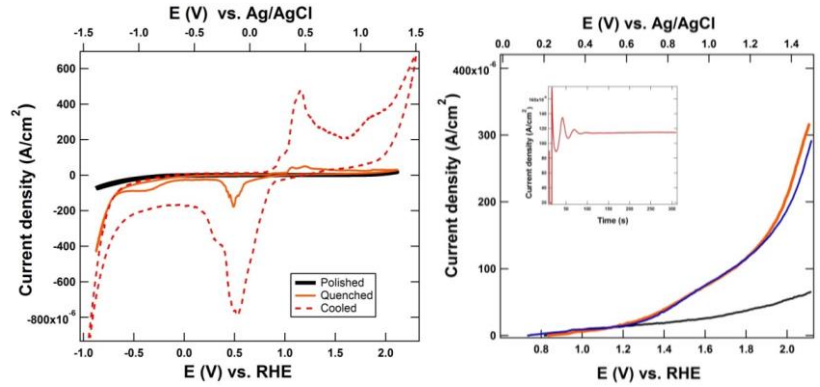

Figure 2.1c. Left: Comparison of CV scans for $LaTiO_2N$ films which were naturally cooled (dashed red), quenched (orange), and both quenched and polished (black). Right: The photoelectrochemical activity for water oxidation of unoptimized and unfunctionalized $LaTiO_2N$ films is significant, and should greatly increase with co-catalyst functionalization.

The presence of large, flat films single crystal substrates of $La_2Ti_2O_7$ and $La_5Ti_5O_{17}$ which can be prepared both with and without epitaxial $LaTiO_2N$ films provide an exceptional opportunity to carry out surface science studies on oxynitride perovskites to better understand how these surfaces interact with water during photoelectrochemical processes, since large-area single crystals of oxynitride compounds cannot typically be prepared. Spectroscopic studies of the bare surfaces have been carried out, as well as temperature-programmed desorption (TPD) studies of water binding. Both XPS and STEM/EELS spectroscopy studies find evidence for the partial reduction of Ti^{4+} in $LaTiO_2N$, especially near the sample surface, in a manner that it consistent with the surface decomposition processes described above. However, the estimates of Ti valence obtained from XPS spectra using conventional oxide analysis methods are very inconsistent with the chemical composition of this phase (average Ti valence of 3.25 – 3.41), suggesting that the influence of N^{3-} anions on the spectra is significant and is not well understood. Further excited-state theoretical studies are needed to effectively interpret the unusual XPS spectra for this phase.

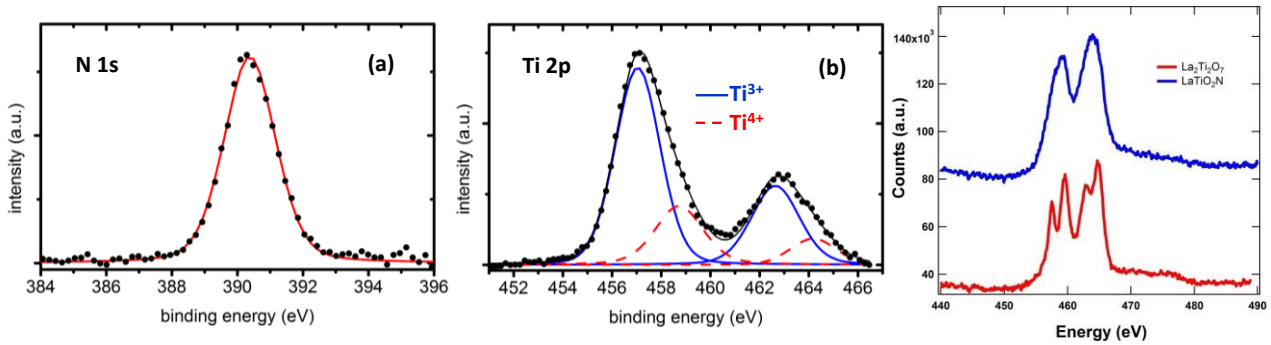

Figure 2.1d. $LaTiO_2N$ film XPS spectrum and fit for N1s (left) and Ti 2p (center) states. The N1s states are consistent with the presence of N^{3-} anions within the crystalline lattice. Two different Ti valence states appear to be present, Ti^{3+} and Ti^{4+}. Surprisingly, the response is dominated by the nominal Ti^{3+} valence state, in contrast to the Ti^{4+} valence expected by charge balance for the $LaTiO_2N$ stoichiometry. This suggests that the response in mixed-anion systems substantially differs from that of pure oxide systems. Further theoretical investigations into these variations in bonding are warranted. Complementary STEM EELS spectra (right) also suggest a mixture of Ti3+ and Ti^{4+} character, though with a stronger Ti^{4+} than Ti^{3+} contribution. A comparison of the stoichiometry and Ti valence inferred from XPS studies for 3 different $LaTiO_2N$ films (slow-cooled, quenched, quenched and polished) is presented in the table below.

$LaTiO_2N$ film on $La_2Ti_2O_7$ substrate	**[La]/([La]+[Ti]) ± 0.04**	**Ti Valence ± 0.06**	**[O]/([N] +[O]) ± 0.06**	**Inferred stoichiometry**
Slow-cooled	0.48	3.25	0.74	$LaTi_{1.08}O_{2.85}N$
Quenched	0.49	3.23	0.74	$LaTi_{1.04}O_{2.85}N$
Polished	0.51	3.41	0.75	$LaTi_{0.96}O_3N$

In summary, effective methods have been developed for preparing high-quality $LaTiO_2N$ films on conductive $La_5Ti_5O_{17}$ substrates that can serve as photoanodes for photoelectrochemical water oxidation. One paper has been written by the post-doc who completed this comprehensive, interdisciplinary study, and it is presently being finalized for submission. Our approach to this system integrates expertise that we have developed in single crystal growth, thin film growth, and thin film post-processing. Through this work, LTON films have been fully optimized for

light harvesting, as their band gap is optimally matched with the incident solar spectrum and the film thicknesses have been optimized based on the absolute absorption coefficients that we have measured for this system. The next step is to optimize the co-catalyst functionalization and the solution conditions to maximize the catalytic activity for water oxidation. Since the preliminary tests described here were done without a water oxidation co-catalyst, and since good water oxidation catalysts have previously been identified based on studies of powder samples, this next step is highly likely to be successful.

3. Overall context of work.

In order to realize the long-term programmatic goal of solar water splitting with high overall efficiency, this project has focused on the understanding and improvement of semiconductor light absorbers, which are likely to play a key role in applications of this technology due to their potential ability (1) to strongly absorb light, (2) to effectively transport charge carriers, and (3) to be able to operate without decomposition for long periods of time. Oxynitride semiconductors typically have band gaps which are ~0.75 eV smaller than those of oxide analogues, and therefore offer many advantages to meet goal (1) – something that is nearly impossible for conventional oxide semiconductors. The charge transport and stability of oxynitride semiconductors are generally poorly understood. In this work, we demonstrate that the facile nature of N_2 loss from the lattice represents a key chemical reaction which must be monitored during both the sample synthesis and post-processing. This oxidation reaction naturally leads to the reduction of the lattice, and as such can be exploited to reduce the carrier concentration in n-type oxynitride semiconductors (as we have done here), or to alternatively generate p-type semiconductors if the as-prepared oxynitride phase is charge-compensated (as has been seen for other oxynitride semiconductors). We have demonstrated that goal (2) can be met in $(GaN)_{1-x}(ZnO)_x$ semiconductors, as we have for the first time demonstrated methods for quantitatively controlling the free carrier concentration in this landmark semiconductor system for water splitting. Finally, our ability to produce high quality epitaxial thin films of $LaTiO_2N$ thin films suitable for surface science studies provides a unique ability to study the surface decomposition processes relevant to goal (3). As such, the work carried out on this project represents great progress towards the goal of developing oxynitride semiconductors for solar fuel production, though the complexity of this family of compounds will require extensive further study before this class of compounds can be fully exploited for this important application.